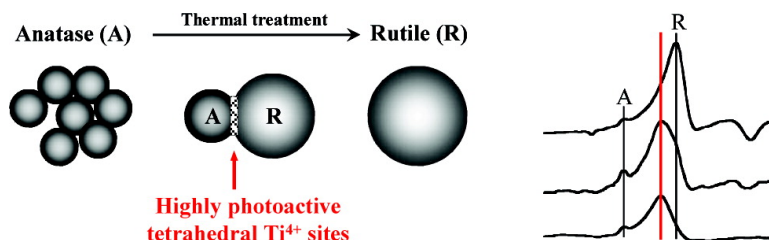


## The Important Role of Tetrahedral Ti Sites in the Phase Transformation and Photocatalytic Activity of TiO<sub>2</sub> Nanocomposites

Gonghu Li, Nada M. Dimitrijevic, Le Chen, Jamie M. Nichols, Tijana Rajh, and Kimberly A. Gray

*J. Am. Chem. Soc.*, **2008**, 130 (16), 5402-5403 • DOI: 10.1021/ja7111118u • Publication Date (Web): 28 March 2008

Downloaded from <http://pubs.acs.org> on February 8, 2009



### More About This Article

Additional resources and features associated with this article are available within the HTML version:

- Supporting Information
- Links to the 2 articles that cite this article, as of the time of this article download
- Access to high resolution figures
- Links to articles and content related to this article
- Copyright permission to reproduce figures and/or text from this article

[View the Full Text HTML](#)

## The Important Role of Tetrahedral $\text{Ti}^{4+}$ Sites in the Phase Transformation and Photocatalytic Activity of $\text{TiO}_2$ Nanocomposites

Gonghu Li,<sup>†</sup> Nada M. Dimitrijevic,<sup>‡</sup> Le Chen,<sup>†</sup> Jamie M. Nichols,<sup>†</sup> Tijana Rajh,<sup>‡</sup> and Kimberly A. Gray<sup>\*,†</sup>

*Institute for Catalysis in Energy Processes, Department of Civil and Environmental Engineering, Northwestern University, Evanston, Illinois 60208, and Chemical Sciences and Engineering Division, Center for Nanoscale Materials, Argonne National Laboratory, Argonne, Illinois 60439*

Received December 14, 2007; E-mail: k-gray@northwestern.edu

Photocatalysis on the surface of semiconductors, particularly  $\text{TiO}_2$ , is among the most promising technologies for converting solar into chemical energy.<sup>1</sup> In photocatalytic processes such as the reduction of  $\text{CO}_2$  to  $\text{CH}_4$  and  $\text{CH}_3\text{OH}$ , isolated tetrahedral  $\text{Ti}^{4+}$  sites are more active than octahedrally coordinated  $\text{Ti}^{4+}$  as in bulk  $\text{TiO}_2$ .<sup>2</sup> The 4-fold  $\text{Ti}^{4+}$  species are usually prepared in confined environment, such as zeolite cavities, or dispersed onto silica substrate.<sup>3</sup> Here, we provide direct evidence for the evolution of tetrahedral  $\text{Ti}^{4+}$  sites in  $\text{TiO}_2$  nanocomposites during the phase transformation from anatase to rutile.

Our previous studies using electron paramagnetic resonance (EPR) spectroscopy revealed the existence of highly distorted, tetrahedral  $\text{Ti}^{4+}$  sites in Degussa P25, a commercial mixed-phase  $\text{TiO}_2$  material consisting of anatase and rutile.<sup>4</sup> However, the origin of such sites in P25 remains elusive. On the basis of the difference between the crystal structures of anatase and rutile, Depero suggested that anatase-to-rutile transformation may require the tetrahedral distortion of octahedral Ti atoms.<sup>5</sup> We hypothesize that the tetrahedral  $\text{Ti}^{4+}$  sites in P25 are generated during the material synthesis at high temperature, which may induce the phase transformation. In this study, the evolution of tetrahedral  $\text{Ti}^{4+}$  sites in P25 after thermal treatment was studied with EPR spectroscopy, which enables an unambiguous identification of reactive electron-trapping sites.<sup>6</sup> We then verified that similar phenomena occurred in the thermal treatment of  $\text{TiO}_2$  prepared by a solvothermal method.

Figure 1 shows the EPR spectra of P25 samples in dark following room-temperature photoexcitation. A resonance at  $g = 1.979$ , which is characteristic of electrons trapped in tetrahedral  $\text{Ti}^{4+}$  sites,<sup>4</sup> is the most prominent electron signal in the EPR spectrum of untreated P25 (Figure 1a). Electrons trapped in anatase lattice and at anatase surface sites are characterized by the EPR signatures having  $g_{\perp} = 1.990$  and  $g_{\parallel} = 1.930$ , respectively, which are also seen in Figure 1a. The resonances associated with electrons trapped in rutile lattice ( $g_{\perp} = 1.975$  and  $g_{\parallel} = 1.947$ ) are clearly seen in the spectrum of P25 sintered at 773 K (Figure 1b). The same EPR spectrum also highlights the evolution of more tetrahedral  $\text{Ti}^{4+}$  sites upon sintering at 773 K, as the corresponding electron signal at  $g = 1.979$  is more intense than that in Figure 1a. Such change in signal intensity is further demonstrated in the EPR spectra acquired under additional UV/visible light illumination at 5 K

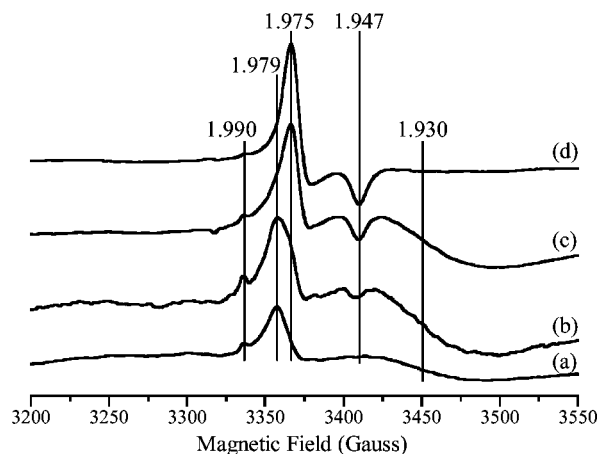


**Figure 1.** EPR spectra of P25 materials: (a) as received, (b) sintered at 773 K, (c) 873 K, and (d) 973 K. The spectra were acquired in the dark at 5 K after illuminating the samples with UV/visible light at 293 K in the presence of 2,4,6-trichlorophenol (TCP). In the EPR experiments, TCP serves as a hole scavenger, minimizing electron-hole recombination and allowing for the accumulation of trapped electrons in  $\text{TiO}_2$ .<sup>4</sup> The spectra have been normalized as explained in Figure S1.

(Figure S1 in Supporting Information). The increase in tetrahedral  $\text{Ti}^{4+}$  sites coincided with measurable increase in the photoactivity of P25 after sintering at 773 K (Figure S2).

While EPR studies revealed the significant development of rutile lattice trapping sites in P25 after sintering at 773 K, X-ray diffraction (XRD) as a bulk technique detected only negligible change in rutile proportion (Figure S3). These results suggest that, in addition to tetrahedral  $\text{Ti}^{4+}$  sites, sintering at 773 K resulted in the formation of small domains of rutile-like clusters instead of bulk rutile phase.

The tetrahedral  $\text{Ti}^{4+}$  signal became less intense in the spectrum of P25 sintered at 873 K, the temperature at which significant phase transformation from anatase to rutile occurred (Figure S3). This is accompanied by the further development of rutile electron signatures in the spectrum shown in Figure 1c. The absence of a strong signal at  $g = 1.979$  in Figure 1d indicates that tetrahedral  $\text{Ti}^{4+}$  sites do not exist in large quantity in P25 after thermal treatment at 973 K.

Thus, tetrahedral  $\text{Ti}^{4+}$  species is an intermediate formed during the anatase-to-rutile transformation induced by thermal treatment. Banfield and co-workers demonstrated that high concentration of nucleation sites for the phase transformation

<sup>†</sup> Northwestern University.

<sup>‡</sup> Argonne National Laboratory.

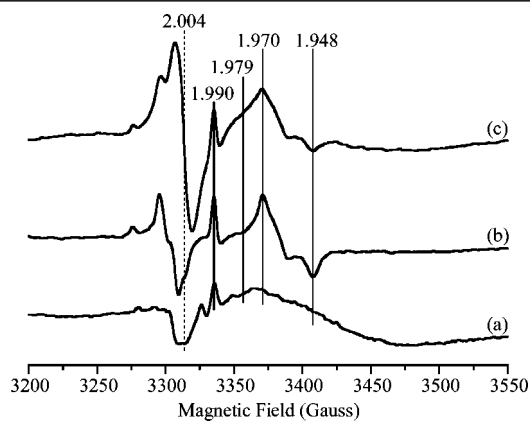


**Figure 2.** EPR spectra of (a) pure-phase anatase  $\text{TiO}_2$  in water, (b) mixed-phase  $\text{TiO}_2$  in water, and (c) mixed-phase  $\text{TiO}_2$  in TCP. The spectra were acquired at 5 K under UV/visible light irradiation. The signal at  $g = 2.004$  is characteristic of phenoxyl radicals.<sup>4</sup> Resonances corresponding to oxygen-centered surface hole sites are seen at  $g = 2.008$ , 2.013, and 2.025 (not labeled).<sup>4</sup>

of anatase to rutile exists at particle–particle interfaces in comparison to bulk materials.<sup>7</sup> Zhang and co-workers proposed that the rutile phase starts to form at the interfaces between the anatase particles during the phase transformation of agglomerated anatase particles.<sup>8</sup> In P25, the tetrahedral  $\text{Ti}^{4+}$  sites were postulated to exist in distorted interfacial region between anatase and rutile.<sup>4</sup>

To probe the relationship between tetrahedral  $\text{Ti}^{4+}$  sites, phase transformation, and reactivity, we further studied anatase and mixed-phase  $\text{TiO}_2$  photocatalysts which were prepared by a solvothermal method followed by thermal treatment at 773 and 873 K, respectively (Figures S4 and S5). Figure 2 shows the EPR spectra of the synthesized materials under illumination.

As can be seen from Figure 2a, the EPR spectrum of the pure-phase anatase dispersed in water exhibits a broad resonance with  $g \sim 1.950$  in addition to the well-resolved signal from anatase lattice trapped electrons ( $g_{\perp} = 1.990$ ). The presence of this broad, unresolved signal indicates the existence of clusters on the anatase surface that have altered Ti symmetry from  $D_{2d}$  (anatase) to rutile-like ( $D_{2h}$ ) or to tetrahedral  $\text{Ti}^{4+}$  species. Clusters with rutile-like character are thought to occur at some fraction of random anatase–anatase particle contacts during the phase transformation.<sup>9</sup>

In the EPR spectrum of the mixed-phase  $\text{TiO}_2$  in water (Figure 2b), rutile lattice signals are seen at  $g_{\perp} = 1.970$  and  $g_{\parallel} = 1.948$ , together with the anatase lattice signature. When the mixed-phase  $\text{TiO}_2$  was illuminated with UV/visible light in the presence of TCP, a broad signal due to trapped electrons around  $g = 1.979$  was also observed (Figure 2c). This broad signal is likely associated with trapped electrons in tetrahedral  $\text{Ti}^{4+}$  sites in the mixed-phase  $\text{TiO}_2$  obtained upon sintering at 873 K. It is not clear whether tetrahedral  $\text{Ti}^{4+}$  sites exist in the “pure” anatase sample since a resonance around  $g = 1.979$  cannot be resolved from the broad signal at  $g \sim 1.950$ , as shown in Figure 2a.

Although the specific surface area of the anatase  $\text{TiO}_2$  is about eight times greater than that of the mixed-phase  $\text{TiO}_2$ , the mixed-phase materials exhibited much higher photocatalytic activity. The photocatalytic degradation of phenol and methylene blue occurred on the mixed-phase  $\text{TiO}_2$  about twice as fast as on the

anatase  $\text{TiO}_2$  (Figure S6). We believe that the tetrahedral  $\text{Ti}^{4+}$  sites contribute to the increased photoactivity of the mixed-phase material relative to the pure-phase anatase. The existence of tetrahedral  $\text{Ti}^{4+}$  sites may also account for the unique properties of mixed-phase  $\text{TiO}_2$ , relative to pure-phase materials, as catalyst support.<sup>10</sup>

In summary, our study confirmed the intermediacy of tetrahedral  $\text{Ti}^{4+}$  sites in the phase transformation from anatase to rutile. Our results also demonstrated an alternate synthesis of such  $\text{Ti}^{4+}$  sites, which are usually prepared in zeolite cavities or dispersed onto silica substrate. In this alternate synthesis, thermal treatment at elevated temperatures induced the tetrahedral distortion of Ti atoms, likely located at the interfaces between  $\text{TiO}_2$  nanoparticles. One can expect a mixed-phase nanocomposite with optimized interfacial morphology to act as an effective photocatalytic relay for solar energy utilization, in which bulk  $\text{TiO}_2$  materials harvest the light and the tetrahedral  $\text{Ti}^{4+}$  sites function as catalytic hot spots.

**Acknowledgment.** The authors thank Prof. Joseph T. Hupp and Karen Mulfort of the Chemistry Department at Northwestern University for their help on surface area measurements, and Degussa for their generous donation of Degussa P25. J.M.N. is grateful for the support from the NSEC-RET program at Northwestern University. This work was supported by grants from the U.S. Department of Energy (DE-FG02-03ER15457/A003 and DE-AC02-06CH11357).

**Supporting Information Available:** XRD patterns, photocatalytic activity, and light EPR spectra of P25 samples; characterization and photocatalytic activity of synthesized anatase and mixed-phase  $\text{TiO}_2$ . This material is available free of charge via the Internet at <http://pubs.acs.org>.

## References

- (1) (a) Diebold, U. *Surf. Sci. Rep.* **2003**, *48*, 53–229. (b) Carp, O.; Huisman, C. L.; Reller, A. *Prog. Solid State Chem.* **2004**, *32*, 33–177. (c) Hirakawa, T.; Kamat, P. V. *J. Am. Chem. Soc.* **2005**, *127*, 3928–3934. (d) Thompson, T. L.; Yates, J. T., Jr. *Chem. Rev.* **2006**, *106*, 4428–4453. (e) Livraghi, S.; Paganini, M. C.; Giamello, E.; Selloni, A.; Di Valentin, C.; Pacchioni, G. *J. Am. Chem. Soc.* **2006**, *128*, 15666–15671. (f) Chen, X.; Mao, S. S. *Chem. Rev.* **2007**, *107*, 2891–2959.
- (2) (a) Zhang, J. L.; Hu, Y.; Matsuoka, M.; Yamashita, H.; Minagawa, M.; Hidaka, H.; Anpo, M. *J. Phys. Chem. B* **2001**, *105*, 8395–8398. (b) Anpo, M.; Takeuchi, M. *J. Catal.* **2003**, *216*, 505–516. (c) Anpo, M.; Thomas, J. M. *Chem. Commun.* **2006**, 3273–3278. (d) Anpo, M.; Shima, T.; Fujii, T.; Suzuki, S.; Che, M. *Chem. Lett.* **1987**, *16*, 1997–2000.
- (3) (a) Lin, W.; Frei, H. *J. Am. Chem. Soc.* **2005**, *127*, 1610–1611. (b) Lin, W.; Han, H.; Frei, H. *J. Phys. Chem. B* **2004**, *108*, 18269–18273. (c) Liu, Z.; Davis, R. J. *J. Phys. Chem.* **1994**, *98*, 1253–1261. (d) Grunwaldt, J. D.; Beck, C.; Stark, W.; Hagen, A.; Baiker, A. *Phys. Chem. Chem. Phys.* **2002**, *4*, 3514–3521. (e) Notari, B.; Willey, R. J.; Panizza, M.; Busca, G. *Catal. Today* **2006**, *116*, 99–110.
- (4) (a) Hurum, D. C.; Gray, K. A.; Rajh, T.; Thurnauer, M. C. *J. Phys. Chem. B* **2005**, *109*, 977–980. (b) Hurum, D. C.; Agrios, A. G.; Gray, K. A.; Rajh, T.; Thurnauer, M. C. *J. Phys. Chem. B* **2003**, *107*, 4545–4549.
- (5) Depero, L. E. *J. Solid State Chem.* **1993**, *104*, 470–475.
- (6) (a) Berger, T.; Sterrer, M.; Diwald, O.; Knozinger, E.; Panayotov, D.; Thompson, T. L.; Yates, J. T. *J. Phys. Chem. B* **2005**, *109*, 6061–6068. (b) Dimitrijevic, N. M.; Saponjic, Z. V.; Rabatic, B. M.; Rajh, T. *J. Am. Chem. Soc.* **2005**, *127*, 1344–1345.
- (7) (a) Banfield, J. F.; Bischoff, B. L.; Anderson, M. A. *Chem. Geol.* **1993**, *110*, 211–231. (b) Gilbert, B.; Zhang, H.; Huang, F.; Finnegan, M. P.; Waychunas, G. A.; Banfield, J. F. *Geochem. Trans.* **2003**, 20–27. (c) Zhang, H.; Banfield, J. F. *Chem. Mater.* **2005**, *17*, 3421–3425. (d) Zhang, H.; Banfield, J. F. *J. Phys. Chem. C* **2007**, *111*, 6621–6629.
- (8) Zhang, J.; Li, M.; Feng, Z.; Chen, J.; Li, C. *J. Phys. Chem. B* **2006**, *110*, 927–935.
- (9) Penn, R. L.; Banfield, J. F. *Am. Mineral.* **1999**, *84*, 871–876.
- (10) Panpranot, J.; Kontapakdee, K.; Praserttham, P. *J. Phys. Chem. B* **2006**, *110*, 8019–8024.

JA711118U